

Fatigue Life Evaluation of TIG-weld of Reduced Activation Ferritic/Martensitic Steel F82H by Small Specimen Test Technique

S. Nogami¹, Y. Sato¹, A. Hasegawa¹ and H. Tanigawa²

¹*Department of Quantum Science and Energy Engineering, Tohoku University, 6-6-01-2, Aramaki-aza-Aoba, Aoba-ku, Sendai 980-8579, Japan*

²*Japan Atomic Energy Agency, 2-4, Shirakata Shirane, Tokai, Naka, Ibaraki 319-1195, Japan*

(Received: 27 October 2009 / Accepted: 14 February 2010)

Evaluation of the low cycle fatigue life by the small specimen test technique (SSTT) and some other properties (metallographical structure and Vickers hardness) for the TIG (tungsten inert gas) weld of F82H IEA-heat were carried out. The TIG-weld was distinguished into seven regions with different metallographical structure and hardness, which were the base metal (BM) region (region with almost no thermal history in the weld), three regions of the heat affected zone (HAZ), and the three regions of the weld metal. There seemed to be no significant correlation between Vickers hardness and average prior austenitic grain size of the individual regions of the TIG-weld. The region with larger prior austenitic grain than the base metal showed similar fatigue life to the BM and the raw material (material used for the TIG-weld). While, the region with relatively small prior austenitic grain showed longer fatigue life than it.

Keywords: Reduced activation ferritic/martensitic steel, F82H, TIG weld, Low cycle fatigue, Life evaluation, Base metal, Heat affected zone, Weld metal, Small specimen test technique

1. Introduction

Reduced activation ferritic/martensitic (RAFM) steel such as F82H and EUROFER has been developed as a primary candidate structural material for a fusion reactor blanket [1]. Since welding is an inevitable procedure for the fabrication of blanket components, and welding region often becomes the weakest part of the component, evaluation of strength and life of the weld should be carried out for developing the reliable component.

Since the fusion reactor structural material must support dynamic loads induced by thermal and electromagnetic stresses, the fatigue life of the RAFM steel and its weld should be clarified. The fatigue life of TIG (tungsten inert gas) weld of F82H evaluated using a standard-size round-bar joint specimen was reported by Kim [2]. Because there was significant difference of the hardness and stress-strain relation among the base metal (BM, region with almost no thermal history in the weld), heat affected zone (HAZ) and weld metal (WM) of that weld, the actual generated strains on the individual regions were different from the controlled nominal value for the specimen. Consequently, fatigue crack initiated at the region where the highest strain was generated.

The objective of this study is to investigate the low cycle fatigue life of the individual regions (BM, HAZ and WM) of the TIG-weld of F82H. In order to avoid the technical issue on the fatigue life evaluation of the weld described above, small specimen test technique (SSTT)

author's e-mail: shuhei.nogami@qse.tohoku.ac.jp

using a miniature hourglass fatigue specimen was applied in this study. By using this specimen, fatigue crack initiation point could be limited to the minimum cross-section, and material at the minimum cross-section could be limited to one individual region of the weld.

2. Experimental Procedure

2.1 Material

Reduced activation ferritic/martensitic steel, F82H IEA-heat was employed as a raw material (material used for the TIG-weld) in this study. The chemical composition of F82H IEA-heat is shown in Table 1. This material was normalized at 1040°C for 40 min and tempered at 750°C for 1 hour. The chemical composition of wire used in the TIG-welding is also shown in Table 1. Post weld heat treatment was performed at 720°C for 1 hour. The detail of welding condition was reported in the open literature [3].

2.2 Metallographical analysis

Metallographical observation was performed by using an optical microscope. Electrolytic polishing of the cross-sectional surface of the TIG-weld after mechanical polishing was performed for the observation using a mixture of acetic acid and perchloric acid.

2.3 Vickers hardness measurement

Vickers hardness measurement of the cross-sectional surface of the TIG-weld was performed using a Vickers

Table 1 Chemical composition of F82H IEA-heat raw material and TIG wire of its weld (unit: wt.%)

	Fe	C	Si	Mn	Cr	Mo	W	V	Ta
Raw material	Bal.	0.09	0.07	0.1	7.84	0.003	1.98	0.19	0.04
TIG wire	Bal.	0.07	0.11	0.52	7.46	<0.005	2.00	0.20	0.02

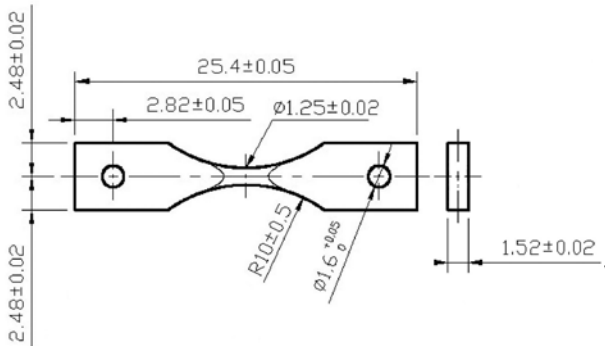


Fig. 1 Shape and geometry of miniature hourglass fatigue specimen

hardness tester (Shimadzu Corp., Micro Hardness Tester HMV-1 TADW). The test temperature, indentation load and dwell time were room temperature, 1.96 N and 15 sec, respectively.

2.4 Low cycle fatigue test

Fig. 1 shows the shape and geometry of miniature hourglass fatigue specimen used in this study. The diameter of the minimum cross-section and the curvature of the hourglass region were 1.25 mm and 10.0 mm, respectively. This specimen is the current standard miniature fatigue specimen in Japan to evaluate the fatigue life of the RAFM steel [4-9]. The specimen was machined perpendicular to the welding line. Seven kinds of the miniature hourglass fatigue specimens were fabricated, which had the BM region, three regions of the HAZ (coarse grain HAZ (CG-HAZ), fine grain HAZ (FG-HAZ) and over-tempered HAZ (Over-tpd. HAZ)), and the three regions of the WM (WM(upper), WM(middle) and WM(bottom)) at the minimum cross section region, respectively. The detail of these seven individual regions is explained in the next chapter.

Fatigue test was carried out at room temperature in air using an electromotive testing machine with a 2 kN load cell fabricated by INTESCO, Japan. The total strain range was controlled using a triangular wave ($R = -1$) with strain rate of about 0.04%/s. The diametral deformation was measured by a laser extensometer. The axial strain range (ϵ_a) was converted from the diametral strain range (ϵ_d) using a conversion equation in ASTM E606 Appendix X2 [10] as follow:

$$\epsilon_a = (\sigma/E)(1 - \nu_e) - 2\epsilon_d \quad (1)$$

where σ , E and ν_e were the axial stress, Young's modulus (217 GPa) and elastic Poisson's ratio (0.3), respectively. The axial total strain range ($\Delta\epsilon_t$) was 1.0% and 2.0% in this study, where plastic deformation occurred during the test in all the specimens of the TIG-weld.

3. Result and Discussion

3.1 Metallographical character

Fig. 2 and Fig. 3 shows metallographical structure of the TIG-weld of F82H IEA-heat and the average prior austenitic grain size of the individual regions of the weld. The average prior austenitic grain size was evaluated based on the ASTM E112-85 [11] using an optical microscope image. As shown in Fig. 2 (a), the TIG-weld was distinguished into seven regions with different metallographical structures, which were the BM region, three regions of the HAZ, and the three regions of the WM. Difference of the maximum temperature during welding and the cooling rate after welding was considered to influence the metallographical structure of the individual regions of the weld.

As shown in Fig. 2 (b), the BM region contained a prior austenitic grain including a packet, block and lath structures, which was the same as the F82H IEA-heat raw material. The average prior austenitic grain size was about 56 μm .

Fig. 2 (c)~(e) show optical microscope images of three regions of the HAZ with different metallographical structures, which were the CG-HAZ, FG-HAZ and Over-tpd. HAZ. The CG-HAZ was the nearest region to the WM and the Over-tpd. HAZ was the nearest region to the BM. The transformation line of the weld was located between the FG-HAZ and the Over-tpd. HAZ. Difference among these three regions could be recognized by the prior austenitic grain size. The average prior austenitic grain sizes of the CG-HAZ, FG-HAZ and Over-tpd. HAZ were about 25 μm , 5 μm and 68 μm , respectively.

Fig. 2 (f)~(h) show optical microscope images of three regions of the WM with different metallographical structures, which were the WM(upper), WM(middle) and WM(bottom). The WM(upper) and WM(bottom) are the upper side and bottom side of the WM with a few millimeters in depth, respectively. Difference among these three regions could be recognized by the prior austenitic grain size. The average prior austenitic grain sizes of the WM(upper), WM(middle) and WM(bottom) were about 130 μm , 7 μm and 100 μm , respectively.

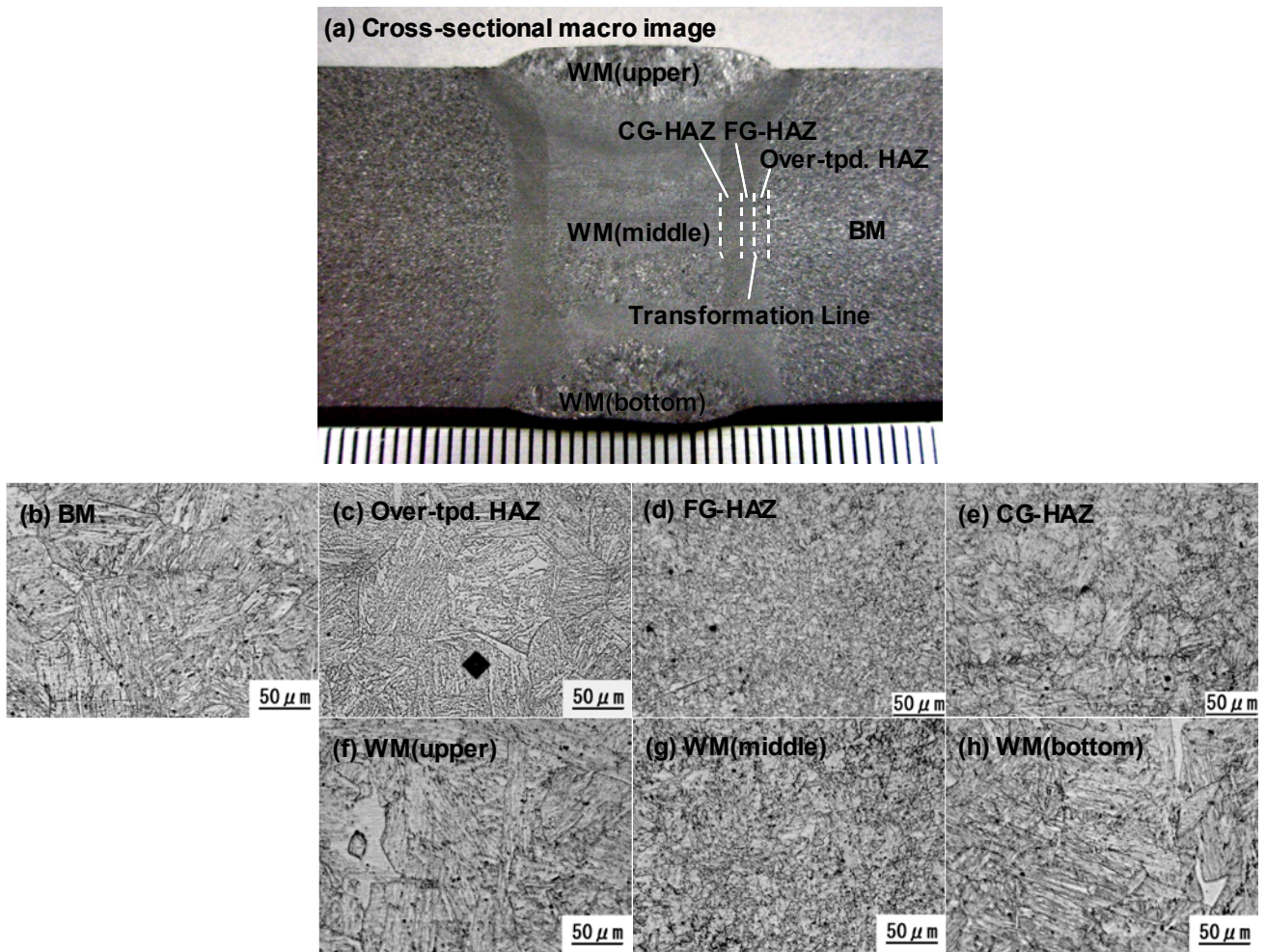


Fig. 2 Metallographical structure of the TIG-weld of F82H IEA-heat. (a) is the whole image of the cross-section and (b)~(h) are high magnification image of the individual regions.

3.2 Vickers hardness

Fig. 4 shows the cross-sectional Vickers hardness distribution of the TIG-weld of F82H IEA-heat. The hardness distribution of the HAZ region was very steep. The lowest hardness was observed in the Over-tpd. HAZ (about 190Hv), which was lower than that of the BM (about 230Hv). While, the highest hardness was observed in the CG-HAZ (about 250Hv), which was higher than that of the BM. The WM(middle) showed almost the same hardness (about 240Hv) as the BM though the metallographical structure was different. The hardness of the WM(upper) and WM(bottom) was the highest among all the regions of the TIG-weld (about 270Hv).

Fig. 5 shows the relation between Vickers hardness and average prior austenitic grain size of the individual regions of the TIG-weld. There seemed to be no significant correlation between them. Since the block and packet size might be different among those individual regions due to the maximum temperature during welding and the cooling rate after welding, the block and packet

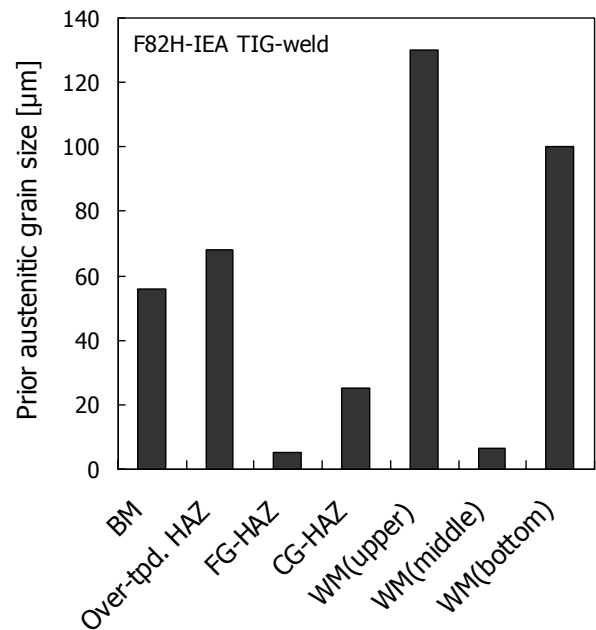


Fig. 3 Average prior austenitic grain size of the individual regions of the TIG-weld of F82H IEA-heat.

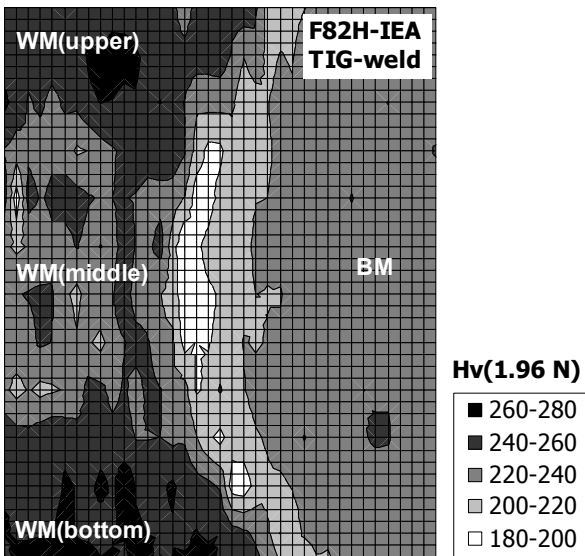


Fig. 4 Cross-sectional Vickers hardness distribution of the TIG-weld of F82H IEA-heat.

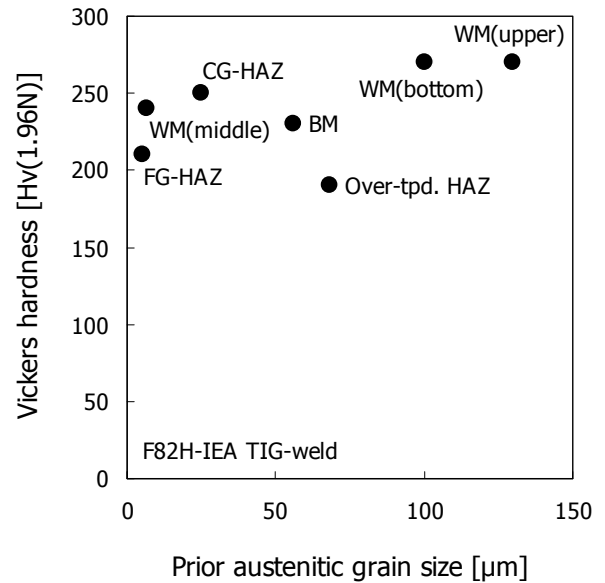


Fig. 5 Relation between Vickers hardness and average prior austenitic grain size of the individual regions of the TIG-weld of F82H IEA-heat.

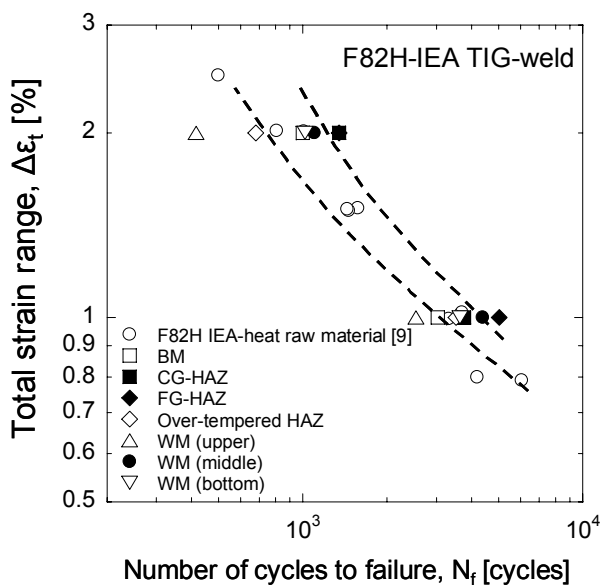


Fig. 6 Relation between total strain range and number of cycles to failure of the individual regions of the TIG-weld of F82H IEA-heat in low cycle fatigue test at room temperature in air [9].

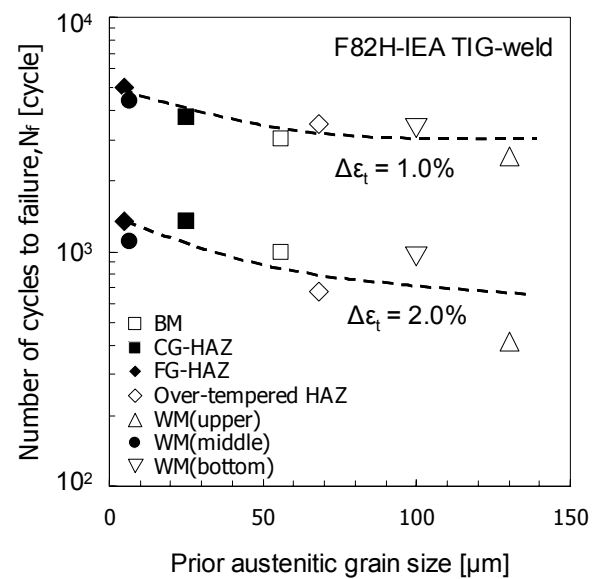


Fig. 7 Relation between number of cycles to failure and average prior austenitic grain size of the individual regions of the TIG-weld of F82H IEA-heat

structure was considered to influence the hardness of them.

3.3 Low cycle fatigue life

Fig. 6 and Fig. 7 show the relation between total strain range and number of cycles to failure, and the relation between number of cycles to failure and average prior austenitic grain size for the individual regions of the TIG-weld of F82H IEA-heat in low cycle fatigue test at

room temperature in air, respectively. The number of cycles to failure (N_f) was defined as the number of cycles at which the tensile peak stress drops to 75% from the extrapolated line of the cyclic softening trend. The fatigue life of the raw material of F82H IEA-heat in Fig. 6 was obtained in the previous study [9]. The region with larger prior austenitic grain than the BM such as the Over-tpd. HAZ, WM(upper) and WM(bottom) showed similar fatigue life to the BM and the raw material. While, the

region with relatively small prior austenitic grain such as the CG-HAZ, FG-HAZ and WM(middle) showed about 1.5~2 times longer fatigue life than it. This tendency was also observed in the previous studies [12, 13], which showed the fatigue life lengthening in martensitic steel by reduction of the prior austenitic grain size. Though the quantitative analysis of this phenomenon is future work, change of the crack growth rate and stress intensity factor due to grain size was considered to be one of the reasons according to the Yokobori's work [14].

4. Summary

Evaluation of the low cycle fatigue life by the SSTT and some other properties (metallographical structure and Vickers hardness) for the TIG-weld of F82H IEA-heat were carried out. The results of this work are summarized as follows:

- (1) The TIG-weld of F82H IEA-heat was distinguished into seven regions with different metallographical structure and hardness, which were the BM region, three regions of the HAZ (CG-HAZ, FG-HAZ and Over-tpd. HAZ), and the three regions of the WM (WM(upper), WM(middle) and WM(bottom)).
- (2) There seemed to be no significant correlation between Vickers hardness and average prior austenitic grain size of the individual regions of the TIG-weld.
- (3) The region with larger prior austenitic grain than the BM such as the Over-tpd. HAZ, WM(upper) and WM(bottom) showed similar fatigue life to the BM and the raw material. While, the region with relatively small prior austenitic grain such as the CG-HAZ, FG-HAZ and WM(middle) showed longer fatigue life than it.

5. References

- [1] R.J. Kurtz, A. Alamo, E. Lucon, Q. Huang, S. Jitsukawa, A. Kimura, R.L. Klueh, G.R. Odette, C. Petersen, M.A. Sokolov, P. Spätig, J.-W. Rensman, *J. Nucl. Mater.*, **386-388**, 411-417 (2009).
- [2] D.H. Kim, Ph'D thesis of Kyoto University, (2008).
- [3] T. Sawai, K. Shiba, A. Hishinuma, *J. Nucl. Mater.*, **283-287**, 657-661, (2000).
- [4] T. Hirose, H. Sakasegawa, A. Kohyama, Y. Katoh, H. Tanigawa, *J. Nucl. Mater.*, **283-287**, 1018-1022 (2000).
- [5] H. Tanigawa, T. Hirose, M. Ando, S. Jitsukawa, Y. Katoh, A. Kohyama, *J. Nucl. Mater.*, **307-311**, 293-298 (2002).
- [6] T. Hirose, H. Tanigawa, M. Ando, A. Kohyama, Y. Katoh, M. Narui, *J. Nucl. Mater.*, **307-311**, 304-307 (2002).
- [7] S.W. Kim, H. Tanigawa, T. Hirose, K. Shiba, A. Kohyama, *J. Nucl. Mater.*, **367-370**, 568-574 (2007).
- [8] S.W. Kim, H. Tanigawa, T. Hirose, A. Kohayama, *J. Nucl. Mater.*, **386-388**, 529-532 (2009).
- [9] S. Nogami, Y. Sato, A. Tanaka, A. Hasegawa, A.

Nishimura, H. Tanigawa, *J. Nucl. Sci. Tech.*, **47-1**, 47-52 (2010).

- [10] ASTM E606, Tentative Recommended Practice for Constant-Amplitude Low-Cycle Fatigue Testing, Annual Book of ASTM, 626-643 (1977).
- [11] ASTM E112-85, Standard Methods for Determining the Average Grain Size, Annual Book of ASTM, 227-290 (1986).
- [12] T. Hayashi, N. Kurasawa, K. Yamada, *JFE Technical Report*, **23**, 4-9, (2009).
- [13] C. Ooki, K. Maeda, H. Nakashima, *NTN Technical Report*, **71**, 2-7, (2003).
- [14] T. Yokobori, A.T. Yokobori, Jr., K. Sato, M. Omotani, *Eng. Fract. Mech.*, **17-1**, 75-85, (1983).

Acknowledgement

Authors are grateful to Prof. A. Kohyama of Kyoto University (Muran Institute of Technology in present) and Prof. T. Hinoki of Kyoto University for their support of installing the fatigue testing machine in Tohoku University.